DOI: 10.1021/ma101227w

Macromolecules
COMMUNICATION TO THE EDITOR

Elucidating the Formation of Block Copolymer Nanostructures on Patterned Surfaces: A Self-Consistent Field Theory Study

Xianggui Ye,[†,‡] Brian J. Edwards,*[,†,‡] and Bamin Khomami*[,†,‡]

[†]*Materials Research and Innovation Laboratory (MRAIL), Department of Chemical and Biomolecular Engineering, University of Tennessee, Knoxville, Tennessee 37996, United States, and* [‡]*Sustainable Energy Education and Research Center, University of Tennessee, Knoxville, Tennessee 37996, United States*

Received June 1, 2010
Revised Manuscript Received September 28, 2010

1. Introduction. Block copolymers (BCPs) are composed of two or more chemically distinct and frequently immiscible blocks that are covalently bonded. Because of thermodynamic incompatibility, distinct blocks will self-organize into different structures via microphase separation. To control these structures, one can tune the composition of the block copolymer or introduce additional distinct blocks into the molecular structure of the macromolecule. Modern synthetic chemistry enables the tailoring of a copolymer's atomistic architecture and hence the equilibrium properties of both the individual blocks and the ensemble.

Chemically patterned substrates can direct the assembly of adsorbed layers or thin films of block copolymers.[1−6] Specifically, recent experimental studies with stripe- and spot-patterned surfaces have demonstrated the ability to induce long-range ordered vertical lamellae and vertical cylinders.[1−4] Moreover, by adjusting the degree of mismatch between the width of the stripe pattern and the natural spacing of the bulk block copolymer, novel morphologies have been created. The computational studies of Daoulas et al.[5,6] have demonstrated the ability to create complex three-dimensional nanostructures from self-assembling block copolymers on two-dimensionally chemically patterned substrates with mismatched symmetry. Thus, it might be possible to create complex three-dimensional nanostructures from by self-assembling block copolymers on one-dimensionally chemically patterned substrates with mismatched symmetry (see Figure 1). In this study, we examine the possibilities for fabrication of complex three-dimensional nanostructures from self-assembly of block copolymers on a one-dimensionally chemically patterned substrate via mismatched symmetry between the stripe patterns.

2. Methodology. In our computations, we have utilized the real-space self-consistent field theory (SCFT), as developed by Drolet and Fredrickson,[7−9] which involves a direct implementation of SCFT in real space in an adaptive, arbitrary cell. The free energy of the system is given as

$$F/nk_BT = -\ln(Q_P/V) + \frac{1}{V}\int d\mathbf{r}\,[\chi_{AB}N\phi_A(\mathbf{r})\phi_B(\mathbf{r}) - w_A(\mathbf{r})\phi_A(\mathbf{r}) - w_B(\mathbf{r})\phi_B(\mathbf{r}) + H(\mathbf{r})(\phi_A(\mathbf{r}) - \phi_B(\mathbf{r})) - P(\mathbf{r})(1 - \phi_A(\mathbf{r}) - \phi_B(\mathbf{r}))] \quad (1)$$

*Corresponding authors. E-mail: bkhomami@utk.edu (B.K.) or bje@utk.edu (B.J.E.).

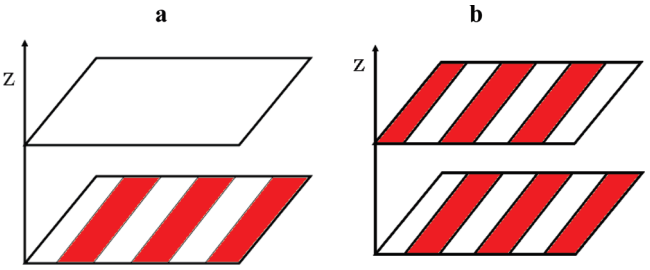

Figure 1. Schematic illustration of the surfaces: (a) the top surface is neutral to both A and B blocks. For the bottom surface, the white region attracts A-blocks and the red region attracts B-blocks. (b) Chemical patterns of both surfaces showing the A-preferring (white) and the B-preferring (red) surface elements. Note the mismatch of stripe symmetry between the top and bottom surfaces.

where $H(\mathbf{r})$ is the polymer−surface interaction, which is assumed to be short-ranged and which has the same units as the Flory−Huggins interaction parameter, χ_{AB}. Specifically, when the simulation cells are adjacent to the patterned surface, $H(\mathbf{r}) = H_A$ or H_B, otherwise, $H(\mathbf{r}) = 0$, and the strength of a lattice relative to the pattern surface (i.e., H_A and H_B) depends on the patterned surface. When $H(\mathbf{r})$ is negative, the surface favors A segments, and when $H(\mathbf{r})$ is positive, the surface favors B segments. $w_A(\mathbf{r})$ and $w_B(\mathbf{r})$ are the mean fields, which are produced by the surrounding chains. $P(\mathbf{r})$ is a Lagrange multiplier (in the form of a pressure) that is used to ensure that the incompressibility condition is satisfied. Minimizing the free energy with respect to the densities and mean fields leads to the SCFT equations

$$\begin{aligned} w_B(\mathbf{r}) &= \chi_{AB}(\phi_A(\mathbf{r}) - f_A) - H(\mathbf{r}) + P(\mathbf{r}) \\ w_A(\mathbf{r}) &= \chi_{AB}(\phi_B(\mathbf{r}) - f_B) + H(\mathbf{r}) + P(\mathbf{r}) \\ \phi_A + \phi_B &= 1 \end{aligned} \quad (2)$$

$$\phi_A = -\frac{V}{Q}\frac{\partial Q_P}{\partial \omega_A} = \frac{V}{Q}\int_0^{f_A} ds\, q(\mathbf{r},s)q^+(\mathbf{r},s)$$

$$\phi_B = -\frac{V}{Q}\frac{\partial Q_P}{\partial \omega_B} = \frac{V}{Q}\int_{f_A}^{1} ds\, q(\mathbf{r},s)q^+(\mathbf{r},s)$$

where $q(\mathbf{r},s)$, and $q^+(\mathbf{r},s)$ denote the end-segment distribution functions, which specify the probability of finding the segment s at a spatial position $\mathbf{r}$. The single-chain partition function, $Q_P = \int d\mathbf{r}\, q(\mathbf{r},1)$, is the partition function of a single diblock copolymer chain in the mean fields w_A and w_B. $q(\mathbf{r},s)$ and $q^+(\mathbf{r},s)$ satisfy the following Fokker−Planck equations and a set of initial conditions

$$\frac{\partial q(\mathbf{r},s)}{\partial s} = \nabla^2 q(\mathbf{r},s) - w(\mathbf{r})q(\mathbf{r},s); \quad q(\mathbf{r},0) = 1 \quad (3)$$

$$-\frac{\partial q^+(\mathbf{r},s)}{\partial s} = \nabla^2 q^+(\mathbf{r},s) - w(\mathbf{r})q^+(\mathbf{r},s); \quad q^+(\mathbf{r},1) = 1 \quad (4)$$

For $0 \le s \le f_A$, $w(\mathbf{r}) = w_A(\mathbf{r})$, and for $f_A \le s \le 1$, $w(\mathbf{r}) = w_B(\mathbf{r})$.

When solving eqs 3 and 4, Dirichlet boundary conditions were used in the z-direction. Specifically, on the surface sites of the confining walls, the end-segment distribution functions and polymer densities are set to be zero.[10,11] Periodic boundary conditions have been used in the other directions.

 Published on Web 11/04/2010

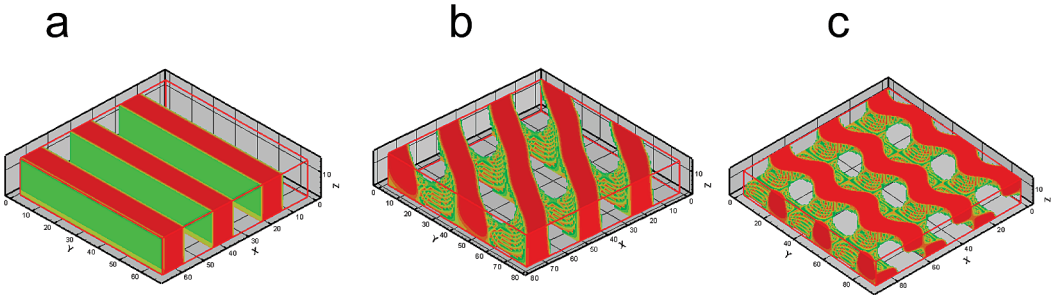

Figure 2. Thin film morphologies of A−B symmetrical diblock copolymer directed by the striped pattern. By increasing the spacing period of the pattern, three different stable morphologies are observed. In the snapshot, only the distribution of block A is shown. The thickness of the film is $2.99R_g$. The spacing periods of the patterns of (a), (b), and (c) are $4.38R_g$, $5.18R_g$, and $5.98R_g$, respectively. The free energies of morphology (b) and (c) are $0.01k_bT$ and $0.20\ k_bT$ per chain lower than those of the stretched lamellar structures, respectively.

The results reported are mostly based on the following discretization: (1) the chain contour length is divided into 200 segments, and (2) the lattice constant is taken as $0.20R_g$, in which R_g represents the unperturbed radius of gyration. Moreover, the width of the pattern L_s is changed by increasing the number of cells corresponding to a given pattern while maintaining the size of the cells at $0.20R_g$.

We have performed simulations with $H = \pm 7.0$ and $\chi_{AB}N = 25.0$. In the white region of the patterned surfaces in Figure 1 H is positive, and in the red region H is negative; otherwise, H is zero. This choice has been motivated by the work of Chen et al.[10] Various runs with different initial fields have been performed, and the morphology with the lowest free energy is concluded to be the most stable phase under the given set of conditions.

3. Results and Discussion. *3.1. Morphologies of a Symmetrical Block Copolymer on a Stripe-Patterned Surface.* In Figure 2, thin film morphologies of an A−B symmetrical diblock copolymer directed by a stripe-patterned surface are displayed. The characteristic spacing of this system in the bulk is $L_0 = 4.21R_g$. It should be noted here that confinement between the plates does not affect the spacing of the lamellae in the perpendicular orientation.[12,13] In this case, there is one alternating chemically striped pattern on the bottom surface, which is shown in Figure 1a, and one neutral surface at the top ($H = 0.0$). For the two surfaces, the alternating chemically striped patterns match the natural spacing of the block copolymer, and the vertical lamellar morphology is observed (shown in Figure 2a). By computing the free energy difference between the standing lamellae (as shown in Figure 2a) and the structure of the two lamellar phases with different orientations (as shown in Figure 2b), Muller et al.[6] found that stretching the lamellar period by 20% is the limit of stability of standing lamellae. However, by increasing the spacing of the striped chemical pattern, the two lamellar phases with different orientations depicted in Figure 2b become the more stable phase, in which the spacing of the morphology at the top surface has been adjusted to be close to that in the bulk. As the film thickness and the degree of mismatch are increased, the double lamellar structure with different length scales and orientations is the most stable morphology. It should be noted that the size of the system also plays a critical role in determining the most stable morphology. Specifically, if the total pattern length of the system is an integer multiple of the bulk period, the resulting morphology will be that of two lamellae with the same orientation.[14]

For a thin film with height of $2.99R_g$, when the periodic spacing is smaller than that of the bulk, after the two lamellar phases with different orientations appear, an increasing degree of mismatch results in two lamellar phases with the same orientation (shown in Figure 2c). Further increase in the chemically stripe-patterned spacing to $1.9L_0$, while keeping the thickness fixed, a structure similar to that of Figure 2c is also found. Undulating interfaces of the A−B block copolymer at the top surface are observed in the morphology (see Figure 2c). The undulation of the top layer has been observed previously by using the more coarse-grained Cahn−Hilliard model at $W = 16$ and $D = 7$ (W is chemical stripe width, D is the film thickness, and the bulk lamellar size is about 15 [in units of Kuhn length]);[15] however, since the transverse direction morphology was not elucidated in this work, it is very difficult to determine the exact morphology of the films.[15]

Table 1. Summary of Morphologies with Different Pattern Periods and Different Film Thicknesses

	L_s/L_0			
thickness (R_g)	1.0	1.2	1.4	1.9
1.99	A[a]	A	B[b]	C[c]
2.99	A	B	C	C
3.59	A	B	B	B
4.38	A	B	B	B

[a] A refers to the perpendicular lamella morphology shown in Figure 2a. [b] B refers to the two lamella structure with different orientations shown in Figure 2b. [c] C refers to the two lamella structure with same orientation shown in Figure 2c.

Tsori and Andelman[16−18] have also observed the tilt lamellar morphology with increasing mismatch degree between the bulk period and the surface chemical-pattern period in the weak segregation region by using a Ginzburg−Landau expansion of the free energy. It should be noted that their calculations are only in the weak segregation region and their films are thicker. It should also be noted that the line tension of the stiff AB interface approaching the surface is minimal when the orientation of the AB interface is locally perpendicular to the surface.[6] Clearly, in a tilt lamellar morphology the polymer chains need to be stretched significantly, especially when the chains are close to the top surface; however, the morphology in Figure 2c (dubbed the "alternating tilt morphology") has a higher entropy than the tilt lamellar morphology because the chains are less stretched. As discussed in the preceding paragraph, in the case of thicker films, the lamellar phases with the same orientation may also appear; however, the lamellar phases with the same orientation only have the same orientation with respect to the substrate, but not the same spatial spacing.

A summary of morphologies with different pattern periods and different film thicknesses is shown in Table 1, where A refers to the perpendicular lamella morphology shown in Figure 2a; B refers to the two lamella structure with different orientations shown in Figure 2b; and C refers to the two

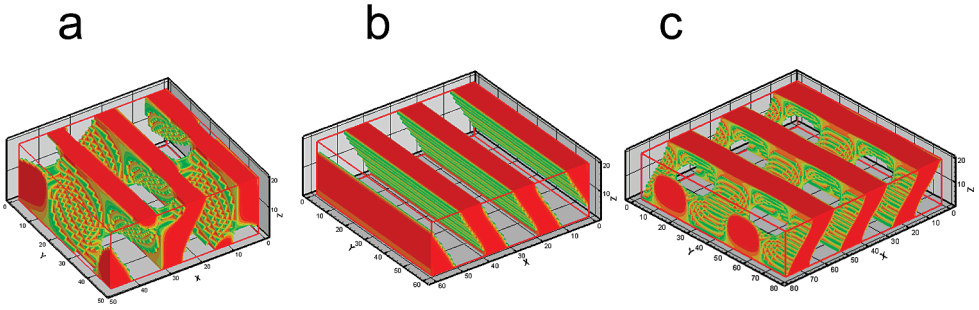

Figure 3. Thin film morphologies of A−B symmetrical diblock copolymer directed by two chemically stripe-patterned surfaces. By increasing the spatial period of the pattern, three different stable morphologies are observed. In the snapshots, only the distribution of the A-block is shown. The thickness of the film is $3.98R_g$. The spacing periods of the pattern of (a), (b), and (c) are $3.19R_g$, $3.98R_g$, and $5.18R_g$, respectively.

lamella structure with same orientation shown in Figure 2c. When the thickness of the film is $1.99R_g$, the morphology change as a function of the pattern mismatch (L_s/L_0) is similar to that of the film that is $2.99R_g$ thick. However, upon further increase in the film thickness to $3.59R_g$ and $4.38R_g$, the morphologies depicted in Figure 2a−c are once again observed, albeit that the structure depicted in Figure 2c is no longer the most stable structure. In fact, the structure shown in Figure 2b is the most stable. This suggests that close to the top surface the block copolymer has adjusted its morphology to a lamellar structure with its bulk period. It should be noted that the structure of Figure 2c may become the most stable morphology again if one keeps on increasing the pattern period for thin film. Nevertheless, the point where the block copolymers begin to form at their natural spacing depends on the degree of mismatch between the chemical-pattern period and the natural spacing of the block copolymer and interaction parameter $\chi_{AB}N$. Therefore, the film morphology can be controlled by proper selection of the film thickness and the level mismatch in the pattern.

To ensure the fidelity of the aforementioned computational results, we have performed simulations with higher degree of discretizations, i.e., chain discretized into 300 segments and a lattice constant of $0.10R_g$. These simulations have clearly demonstrated the robustness of the aforementioned morphologies.

3.2. Morphologies of a Symmetrical Block Copolymer on Two Chemically Stripe-Patterned Surfaces. Figure 1b displays two chemically stripe-patterned surfaces with mismatched symmetry with respect to the one-dimensional spatial period. By increasing the degree of mismatch between the bulk spacing of the block copolymer and the striped pattern width, three different morphologies are observed (see Figure 3). The thickness of the film examined is $3.98R_g$, which is smaller than the bulk spacing of the block copolymer. As evident in Figure 3, the morphology of the block copolymer follows the surface pattern near to the two patterned surfaces. As expected, when the striped pattern period is comparable with the natural spacing of the block copolymer, the tilt morphology is favored. When the mismatch degree between the striped pattern period and the natural period of the block copolymer is significant, bicontinuous network structures are favored, as depicted in Figure 3a,c. Upon close inspection, we note that the two network structures are different. In Figure 3a, the morphology is close to the checkerboard morphology, except that the different regions are connected by bridges.[19] It should be noted that the pattern width is smaller than the natural spacing of the block copolymer. Thus, the preferred orientation of the chains is vertical to the surface; however, in Figure 3c, the morphology resembles the alternating tilt morphology, which was observed in the previous section. The reason for this difference is that the chains are able to lie down on the surface along the boundaries of the different patterns beside the vertically oriented chains relative to the substrate in Figure 3c.

As discussed in the preceding section, the thickness of the film has a significant effect on the morphology for the stripe-patterned surface; the same effect is observed for a system with two stripe-patterned surfaces separated by a fixed spatial distance. In the regions near to the patterned surfaces, the block copolymer follows the patterned surfaces, but with increasing film thickness with the same degree of mismatch between the surface pattern width and the bulk spacing of the block copolymer, the block copolymers adjust to form the lamellar morphology with the bulk spacing in the middle region of the film.

Clearly, the morphology of Figure 3c is bicontinuous with a significant surface area. The size of the channel can be tuned by the pattern size within a specified range, and the perfect match of the BCP morphology with the patterned surfaces provides the potential to tailor the components of the bicontinuous thin film morphologies from the patterned-surfaces substrate and thereby possibly enable connections to technological applications, e.g., filtration, conduction, and high-surface area membranes.

4. Conclusions. Chemically patterned substrates can direct the assembly of adsorbed layers or thin films of block copolymers. Here, we considered the self-assembly of a lamellae-forming diblock copolymer on periodically stripe-patterned substrates. The morphology of the block copolymer follows the pattern at the substrate; however, with an increasing degree of mismatch between the width of the stripe pattern and the periodic spacing of bulk block copolymer, novel morphologies were observed. Therefore, it is possible to adjust the morphologies in thin block copolymer films by adjusting the degree of mismatch between the width of the stripe pattern and the periodic spacing of the bulk block copolymer via judicious selection of the film thickness. These results demonstrate a promising strategy for fabrication of complex interfacial nanostructures from chemically patterned substrates.

Acknowledgment. Funding for this project was provided by the Sustainable Energy Education and Research Center at the University of Tennessee—Knoxville. B.K. thanks NSF for supporting this work through funding Grant CBET-0932666.

References and Notes

(1) Bita, I.; Yang, J. K. W.; Jung, Y. S.; Ross, C. A.; Thomas, E. L.; Berggren, K. K. *Science* **2008**, *321* (5891), 939–943.
(2) Park, S. M.; Craig, G. S. W.; La, Y. H.; Solak, H. H.; Nealey, P. F. *Macromolecules* **2007**, *40* (14), 5084–5094.

(3) Ruiz, R.; Kang, H. M.; Detcheverry, F. A.; Dobisz, E.; Kercher, D. S.; Albrecht, T. R.; de Pablo, J. J.; Nealey, P. F. *Science* **2008**, *321* (5891), 936–939.
(4) Park, S. M.; Craig, G. S. W.; La, Y. H.; Nealey, P. F. *Macromolecules* **2008**, *41* (23), 9124–9129.
(5) Daoulas, K. C.; Muller, M.; Stoykovich, M. P.; Park, S. M.; Papakonstantopoulos, Y. J.; de Pablo, J. J.; Nealey, P. F.; Solak, H. H. *Phys. Rev. Lett.* **2006**, *96* (3), 036104.
(6) Muller, M.; Daoulas, K. C.; Norizoe, Y. *Phys. Chem. Chem. Phys.* **2009**, *11* (12), 2087–2097.
(7) Drolet, F.; Fredrickson, G. H. *Phys. Rev. Lett.* **1999**, *83* (21), 4317–4320.
(8) Drolet, F.; Fredrickson, G. H. *Macromolecules* **2001**, *34* (15), 5317–5324.
(9) Fredrickson, G. H.; Ganesan, V.; Drolet, F. *Macromolecules* **2002**, *35* (1), 16–39.
(10) Chen, P.; Liang, H. J.; Shi, A. C. *Macromolecules* **2008**, *41* (22), 8938–8943.
(11) Meng, D.; Wang, Q. *J. Chem. Phys.* **2007**, *126*, 234902.
(12) Pickett, G. T.; Balazs, A. C. *Macromolecules* **1997**, *30* (10), 3097–3103.
(13) Matsen, M. W.; Bates, F. S. *J. Chem. Phys.* **1997**, *106* (6), 2436–2448.
(14) Wang, Q.; Yan, Q. L.; Nealey, P. F.; de Pablo, J. J. *Macromolecules* **2000**, *33* (12), 4512–4525.
(15) Chen, H.; Chakrabarti, A. *J. Chem. Phys.* **1998**, *108* (16), 6897–6905.
(16) Tsori, Y.; Andelman, D. *Europhys. Lett.* **2001**, *53* (6), 722–728.
(17) Tsori, Y.; Andelman, D. *J. Chem. Phys.* **2001**, *115* (4), 1970–1978.
(18) Tsori, Y.; Andelman, D. *Interface Sci.* **2003**, *11* (2), 259–268.
(19) Wang, Q. *Macromol. Theory Simul.* **2005**, *14* (2), 96–108.